THE JOURNAL OF IMMUNOLOGY

Enhanced T Cell Function in a Mouse Model of Human Glycosylation

George Buchlis, Pamela Odorizzi, Paula C. Soto, Oliver M. T. Pearce, Daniel J. Hui, Martha S. Jordan, Ajit Varki, E. John Wherry and Katherine A. High

J Immunol 2013; 191:228-237; Prepublished online 24 May 2013;
doi: 10.4049/jimmunol.1202905
http://www.jimmunol.org/content/191/1/228

The Journal of Immunology is published twice each month by
The American Association of Immunologists, Inc.,
9650 Rockville Pike, Bethesda, MD 20814-3994.

Print ISSN: 0022-1767 Online ISSN: 1550-6606.

Enhanced T Cell Function in a Mouse Model of Human Glycosylation

George Buchlis,*,† Pamela Odorizzi,* Paula C. Soto,‡ Oliver M. T. Pearce,‡ Daniel J. Hui,† Martha S. Jordan,* Ajit Varki,‡ E. John Wherry,* and Katherine A. High*,†,§

Clinical evidence for a more active immune response in humans compared with our closest hominid relative, the chimpanzee, includes the progression of HIV infection to AIDS, hepatitis B– and C–related inflammation, autoimmunity, and unwanted harmful immune responses to viral gene transfer vectors. Humans have a unique mutation of the enzyme CMP-*N*-acetylneuraminic acid hydroxylase (CMAH), causing loss of expression of the sialic acid Neu5Gc. This mutation, occurring 2 million years ago, likely altered the expression and function of ITIM-bearing inhibitory receptors (Siglecs) that bind sialic acids. Previous work showed that human T cells proliferate faster than chimpanzee T cells upon equivalent stimulation. In this article, we report that Cmah$^{-/-}$ mouse T cells proliferate faster and have greater expression of activation markers than wild-type mouse T cells. Metabolically reintroducing Neu5Gc diminishes the proliferation and activation of both human and murine Cmah$^{-/-}$ T cells. Importantly, Cmah$^{-/-}$ mice mount greater T cell responses to an adenovirus encoding an adeno-associated virus capsid transgene. Upon lymphocytic choriomeningitis virus infection, Cmah$^{-/-}$ mice make more lymphocytic choriomeningitis virus–specific T cells than WT mice, and these T cells are more polyfunctional. Therefore, a uniquely human glycosylation mutation, modeled in mice, leads to a more proliferative and active T cell population. These findings in a human-like mouse model have implications for understanding the hyperimmune responses that characterize some human diseases. ***The Journal of Immunology*****, 2013, 191: 228–237.**

Mammalian cells are coated with a complex layer of glycans that mediate pathogen binding, cell adhesion, cell trafficking, cell signaling, endocytosis, apoptosis, and proliferation (1). Although heterogeneity in the expression and structure of these glycan chains can exist within the same individual and even within the same organ, an interesting species-specific divergence in these sugars was discovered in 1998. Two groups reported the human-specific inactivating mutation of the enzyme CMP-*N*-acetylneuraminic acid hydroxylase (CMAH), which is responsible for the conversion of sialic acid precursor CMP-Neu5Ac to CMP-Neu5Gc by the addition of a single hydrogen atom (2, 3). As a result, Neu5Gc is not synthesized in human cells and is, in fact, immunogenic (4, 5). This mutation appears to have set in motion a series of genetic and biochemical changes in the biology of sialic acids that may contribute to several unique aspects of human biology in health and disease (6, 7).

Of the many functions that sialic acids play in cellular physiology, their role as ligands of inhibitory Siglecs is well recognized. Siglecs, or sialic acid–binding Ig superfamily lectins, are broadly and variably expressed on cellular surfaces of the mammalian immune system and have unique binding preferences for the type of sialic acid and its linkage to the underlying glycan chain (8). Many Siglecs, including CD22 and most of the CD33-related Siglecs, contain ITIMs in their cytoplasmic tails, which, when phosphorylated by Src family kinases, recruit phosphatases that attenuate downstream signaling (9, 10). A number of studies have characterized the inhibitory effects of Siglecs in human (11–15) and murine (16–18) immune systems. Humans lost expression of Siglec-5 on T cells, which potentially occurred as a result of genetic pressure on Siglec loci after the loss of CMAH function and thus the absence of sialic acid ligand Neu5Gc. Subsequent investigation showed that when equivalently stimulated, human T cells proliferate much faster than nonhuman primate (NHP) T cells, and this proliferation can be slowed by expressing Siglec-5 in the human T cells (19, 20).

Interestingly, humans are much more prone to AIDS progression during HIV infection when compared with HIV-infected chimpanzees and West African chimpanzees that are hosts for related simian immunodeficiency viruses. One hypothesis for human progression to AIDS is that enhanced activation of the human immune system in response to HIV eventually leads to exhaustion and death of CD4$^+$ T cells (7). The hepatitis viruses provide another example of differences in immune response; a large proportion of humans infected with hepatitis B or hepatitis C virus progress to chronic active hepatitis, whereas the disease tends to be acute and self-limited in chimpanzees. Even in those unusual cases that progress to chronic infection in hepatitis B virus– and hepatitis C virus–infected chimpanzees, the severity of complications related to these pathologies is reduced compared with

*University of Pennsylvania School of Medicine, Philadelphia, PA 19104; †Division of Hematology, Department of Pediatrics, Children's Hospital of Philadelphia, Philadelphia, PA 19104; ‡Cellular and Molecular Medicine Department, University of California San Diego, La Jolla, CA 92093; and §Howard Hughes Medical Institute, Philadelphia, PA 19104

Received for publication October 18, 2012. Accepted for publication April 9, 2013.

This work was supported by the National Institutes of Health (Grant P01 HL078810 to K.A.H., Grant P01 HL107150 to A.V., and Grant T32-HL07439 to G.B.) and the Howard Hughes Medical Institute.

G.B. wrote the manuscript; G.B., P.O., P.C.S., A.V., E.J.W., and K.A.H. designed experiments; G.B., P.O., P.C.S., O.M.T.P., M.S.J., A.V., E.J.W., and K.A.H. edited the manuscript; O.M.T.P. synthesized Neu5Gc and Neu5Ac sialic acids; M.S.J. assisted with signaling analysis; D.J.H. assisted in sample processing; and G.B., P.O., and P.C.S. performed and analyzed experiments.

Address correspondence and reprint requests to Dr. Katherine A. High, Children's Hospital of Philadelphia, Room 5060, Colket Translational Research Building, 3501 Civic Center Boulevard, Philadelphia, PA 19104. E-mail address: high@email.chop.edu

The online version of this article contains supplemental material.

Abbreviations used in this article: AAV, adeno-associated virus; Ad, adenovirus; CMAH, CMP-*N*-acetylneuraminic acid hydroxylase; KLRG1, killer cell lectin-like receptor G1; LCMV, lymphocytic choriomeningitis virus; NHP, nonhuman primate; WT, wild-type.

humans. Many of the late complications of hepatitis in humans are due to an overactive immune response, and not the cytopathic effect of the virus itself (7). Finally, in recent clinical trials with viral vectors, humans mounted T cell immune responses to adeno-associated viral (AAV)–mediated gene transfer that were unanticipated from preclinical animal studies, even in NHPs that are natural hosts for AAV (21, 22). Attempts by a number of groups at recapitulating these results in mice have been uniformly unsuccessful (21, 23–26). Thus, a human-specific glycosylation mutation that potentially disrupts ITIM-mediated immune suppression is of interest in analyzing humans' unique susceptibility to these immune response–related pathologies.

Recently, a Cmah$^{-/-}$ mouse has been generated to assess the effect of this human enzyme mutation in the context of both normal and disease settings in an animal model (27, 28). Initial studies in these mice showed human-like features such as delayed wound healing and age-related hearing loss, and a human-like muscular dystrophy phenotype following combined mutation of the dystrophin gene (29). Immunologically, these mice seem to have enhanced B cell proliferation and Ab production, which is consistent with the observation that Neu5Gc is physiologically downregulated during normal B cell activation (28). In addition, a recent publication showed a similar downregulation of CMAH function and Neu5Gc levels in activated wild-type (WT) murine T cells (30).

We hypothesized that mice engineered to mimic the human mutation of the Cmah gene would display enhanced T cell responses to in vitro and in vivo stimulation. We found that, upon equivalent T cell stimulation in vitro, Cmah$^{-/-}$ T cells proliferated faster, had greater expression of activation markers, and secreted more IFN-γ than WT T cells. In addition, the responses in both human T cells (which are naturally Cmah deficient) and Cmah$^{-/-}$ mouse T cells were blunted by reintroducing the missing Neu5Gc sialic acid onto the cell surface via metabolic incorporation from the culture media. Immunization of Cmah$^{-/-}$ mice with an adenoviral (Ad) vector encoding the AAV (Ad–AAV) capsid elicited a stronger T cell response in Cmah$^{-/-}$ mice compared with WT littermate mice. Finally, we asked whether the robust T cell immune responses of Cmah$^{-/-}$ mice were seen in the context of a live replicating viral infection. Cmah$^{-/-}$ mice infected with acute lymphocytic choriomeningitis virus (LCMV) strain Armstrong developed more LCMV-specific T cells in the blood and spleen. Importantly, LCMV peptide-stimulated splenic T cells from Cmah$^{-/-}$ mice produced a higher proportion of cytokines than WT T cells at day 42 post-infection. These findings shed light on the role that glycosylation plays in immune regulation, and may give evolutionary insight into the cause of overactive immune pathologies in humans.

Materials and Methods

Mice

Cmah$^{-/-}$ mice generated as described previously (27) and backcrossed to C57BL/6 mice >10 generations were bred with C57BL/6 mice purchased from Jackson Laboratories to obtain heterozygous breeding pairs. Heterozygous breeding pairs were then mated, creating Cmah$^{-/-}$, Cmah$^{+/-}$, and Cmah$^{+/+}$ (essentially WT and will be referred to as such in this article) mice. The Cmah$^{-/-}$ and WT mice were used in experiments as littermates, and surplus Cmah$^{+/-}$ heterozygous mice were saved for future mating. Mice were bred and maintained, and investigations were conducted according to an approved Children's Hospital of Philadelphia Institutional Animal Care and Use Committee protocol.

In vitro proliferation and activation assays

Naive Cmah$^{-/-}$ and WT mouse spleens were harvested, and splenocytes were isolated using a 70-μm nylon cell strainer and plunger. Isolated splenocytes were either directly labeled with Cell Trace CFSE (Invitrogen) and plated in culture, or subjected to CD8$^+$ T cell isolation using the CD8$^+$ T Cell Negative Isolation Kit (Dynal/Invitrogen) and then labeled with CFSE. 2E6 CFSE–labeled cells were plated with 25 μl anti-CD3/anti-CD28 activator beads (Dynal/Invitrogen) in 1 ml AIM V culture medium (Life Technologies) supplemented with 3% FBS, penicillin/streptomycin, and glucose. Cells were cultured in these conditions for 3 or 5 d, harvested, washed, and stained with 1:100 anti–CD62L-PE (BD Bioscience) and 1:100 anti–CD25-allophycocyanin-Cy7 (BD Bioscience) for 30 min at 4˚C. Cells were washed twice, resuspended in 4% paraformaldehyde solution, and read on a FACSCanto II (BD) flow cytometer.

Neu5Gc feeding experiments

Mouse T cell experiments. CFSE (5 μM)-labeled negatively isolated mouse T cells were cultured for 2 d in 6 mM Neu5Gc- or Neu5Ac-containing media, stimulated with immobilized anti-CD3 (200 ng/ml) and soluble anti-CD28 (1 μg/ml), and analyzed for CD69 (anti–CD69-PE; BD) expression and CFSE dilution after 5 d.

Human T cell experiments. Isolated human CD4 T cells were cultured for 3 d in 3 mM Neu5Gc- or Neu5Ac-containing media, stimulated with immobilized anti-CD3 (25 ng/ml) and soluble anti-CD28 (1 μg/ml), and analyzed for CD25 expression after 2 d. For proliferation analysis, human PBMCs were labeled with 5 μM CFSE, stimulated with immobilized anti-CD3 (25 ng/ml) and soluble anti-CD28 (1 μg/ml) for 5 d, and analyzed for CFSE dilution. Neu5Gc and Neu5Ac sialic acid stocks were synthesized as described previously (31).

In vitro stimulation

Isolated splenocytes were plated at either 1E6/200 μl (LCMV and AAV peptide stimulations) or 1E6/500 μl (PMA and anti-CD3 stimulations) and incubated for 5 h in either 10% FBS RPMI (LCMV stimulations; Life Technologies) or 3% FBS AIM V media as described earlier (AAV peptide, PMA, and anti-CD3 stimulations). For PMA, anti-CD3, and AAV peptide stimulations, 1 μl BD GolgiStop (BD) was added to the stimulation medium to block transport and intracellularly accumulate cytokines. For LCMV stimulations, 1:500 GolgiStop and 1:1000 GolgiPlug (BD) were added to the stimulation media, along with 1:1000 anti–CD107a-Alexa Fluor 488 (BioLegend). Stimulant concentrations were as follows: 50 ng/ml PMA along with 1 μg/ml ionomycin, 1 μg/ml anti-CD3, 5μg/ml AAV2 H2K^b peptide (SNYNKSVNV) (32), 0.4 ng/ml LCMV GP276 or GP66-77 peptides.

Intracellular cytokine staining

Surface stains. After 5 h of stimulation, cells were harvested, washed, and surface stained for 30 min at 4˚C. For LCMV stimulations, cells were stained for 20 min at room temperature with 1:600 Live/Dead Fixable Aqua Dead Cell Stain, washed, stained 30 min at 4˚C with 1:400 anti–CD4-PE Texas Red (Invitrogen) or 1:100 anti–CD8-PE Texas Red (Invitrogen) and anti–CD44-Alexa Fluor 700 (BioLegend). For AAV stimulation, cells were stained for 30 min at 4˚C with 1:100 anti–CD8-Pacific Blue (BioLegend) and 1:100 anti–CD44-allophycocyanin-Cy7 (BD). For PMA and anti–CD3 stimulations, cells were stained for 30 min at 4˚C with 1:100 anti–CD8-FITC (BD) and anti–CD4-PE (BD).

Intracellular stains. Cells were washed twice, fixed, and permeabilized with Cytofix/Cytoperm solution (BD) for 20 min at 4˚C. Cells were washed twice with Perm Buffer (BD) and stained for 30 min at 4˚C. For LCMV stimulations, 1:100 anti–IFN-γ–PerCp–Cy5.5 (BioLegend), 1:100 anti–TNF-α–Pacific Blue (BioLegend), 1:20 anti–Mip1α-PE (R&D Systems), and 1:100 anti–IL-2–allophycocyanin (eBioscience). For AAV peptide, PMA, and anti-CD3 stimulations, 1:100 anti–IFN-γ–allophycocyanin (BD) was used. Cells were washed twice with Perm Buffer, resuspended in fixative, and read on either an LSRII (BD) or FACS CantoII.

Viral infections

Four-month-old littermate WT and Cmah$^{-/-}$ mice were injected with either 50 μl/leg i.m. in the quadriceps with 1E9 PFU/mouse (Ad–AAV experiments: Ad human 5 construct encoding the AAV2 capsid proteins as a transgene) (32) or 300 μl i.p. with 2E5 PFU/mouse (LCMV experiments: LCMV strain Armstrong). Mice were bled and sacrificed at day 10 post-immunization (Ad–AAV immunization) or bled weekly until sacrifice at day 42 (LCMV infections). Blood was collected retro-orbitally at various time points via heparinized microcapillary tubes (Fisher Scientific) into 1 ml of 4% sodium citrate and 1 ml 1% RPMI. Spleens were harvested and processed at sacrifice as previously described. Cells were washed and then stained for surface markers.

Longitudinal surface stains and LCMV plaque assays

LCMV experiment stains. PBMCs were stained first for 20 min at room temperature with 1:600 Live/Dead Fixable Aqua Dead Cell Stain, washed,

then stained 30 min at 4˚C with 1:100 anti–KLRG1-FITC (Beckman Coulter), anti–CD4-PE Texas Red (Invitrogen), anti–CD8-Pacific Blue (BioLegend), anti–CD127-PE (BioLegend), anti–CD44-Alexa Fluor 700 (BioLegend), and LCMVGp33 tetramer-allophycocyanin.

AAV experiment stains. PBMCs were stained 30 min at 4˚C with 1:10 AAV-SNYNKSVNV Pentamer (Proimmune), 1:100 anti–CD8-Pacific Blue (BioLegend), and 1:100 anti–CD44-allophycocyanin-Cy7 (BD). Cells were then washed twice, resuspended in fixative, and read on either an LSRII or FACS CantoII.

LCMV plaque assays. Spleen homogenates were titered for viral load using a Vero cell plaque assay as previously described (33).

Ly5.2 donor CD8 transfer into Ly5.1 recipient mice

Spleens were harvested from both Cmah$^{-/-}$ and WT mice, and processed as previously described to obtain splenocytes. CD8 T cells were negatively isolated from mouse strain pooled splenocyte populations using the Dynal CD8 negative isolation kit. Because Cmah$^{-/-}$ mice are on a C57BL/6 WT background, they express the Ly5.2 isoform of CD45. We are thus able to transfer these cells into congenic recipient mice expressing Ly5.1 to track donor cells. Four- to 6-wk-old female Ly5.1 mice were purchased from either the National Cancer Institute or Jackson Laboratories to be used as recipient mice. 20E6 Ly5.2 naive donor (Cmah$^{-/-}$ or WT) CD8 T cells were suspended in 200 μl RPMI and injected i.v. into the tail vain of recipient mice. Recipient mice were also infected with LCMV. Mice were bled and sacrificed at days 6–7, and PBMCs and spleens were collected. Splenocytes and PBMCs were stained with the standard panel described in the longitudinal surface stain methods.

Gating strategy for flow cytometric analysis

General gating schemes for the live viral infection analyses throughout this article are described in Supplemental Fig. 1. In brief, cells were plotted forward scatter area versus side scatter area to determine the lymphocyte population. After gating on the lymphocyte population, gates were subsequently made to only include singlets and were further gated on live cells. Then CD8^{+} cells were selected and either plotted for tetramer response or for cytokine analysis and IFN-γ production.

Statistical analysis

All statistical analysis was performed in GraphPad Prism software, and data significance was determined by two-tailed Student *t* test.

Results

In vitro T cell proliferation and activation is augmented in Cmah$^{-/-}$ mice

To assess T cell proliferation and activation in vitro, we isolated both Cmah$^{-/-}$ and WT splenocytes from naive mice. We labeled total splenocytes with CFSE and plated them with anti-CD3/anti-CD28 activator beads for 5 d. By day 5, Cmah$^{-/-}$ CD8 T cells within the splenocyte population proliferated faster than their WT counterparts (Fig. 1A), as did CD4 T cells (Supplemental Fig. 2A). In addition to the observed enhanced dilution of CFSE, division and proliferation indices at 5 d were significantly greater in Cmah$^{-/-}$ CD8 T cells when compared with WT CD8 T cells (Fig. 1B). Unstimulated splenocytes showed no difference in CFSE dilution after 5 d (Supplemental Fig. 2C). This apparent difference in proliferation was not due to potential survival effects of the *Cmah* mutation, as both WT and Cmah$^{-/-}$ cultures had similar levels of cell death when compared with the expected number of cells at 5 d (Supplemental Fig. 2F). In addition, both Cmah$^{-/-}$ CD8 and CD4 T cells had lower levels of CD62L (L-selectin) than WT T cells, the loss of which is a hallmark of T cell activation (Fig. 1A, 1B). Baseline levels of unstimulated CD8 and CD4 T cells showed no difference in CD62L levels (Supplemental Fig. 2D and data not shown). To determine whether the heightened activation and increased proliferation in Cmah$^{-/-}$ T cells was an intrinsic cell phenomenon or was dependent on the context of other splenic populations, we negatively isolated CD8 T cells from naive spleens of both Cmah$^{-/-}$ and WT mice. These CD8 T cells were CFSE labeled, plated at equal numbers, and activated for either 3 or 5 d with anti-CD3/anti-CD28 activator beads. Cmah$^{-/-}$ CD8 T cells had lower levels of CD62L and higher expression of IL-2Rα (CD25), which is upregulated during T cell activation. These differences emerged as early as day 3 poststimulation and were sustained through day 5 (Fig. 1C). Although there was a subtle increase in Cmah$^{-/-}$ CD8 T cell proliferation at day 3, they had proliferated to a much greater extent than WT CD8 T cells by day 5 (Fig. 1C). To investigate whether the enhanced activation and proliferation observed in Cmah$^{-/-}$ versus WT CD8 T cells are associated with early signaling/activation differences, we evaluated CD62L and CD25 expression at early time points after TCR and CD28 stimulation. As early as 5 h postactivation, there were significantly higher frequencies of Cmah$^{-/-}$ T cells that lost CD62L expression when compared with WT littermate CD8 T cells (Fig. 1D). In addition, Cmah$^{-/-}$ CD8 T cells had higher levels of CD25 expression on their surface at 5 h (Fig. 1D). To assess whether these differences in proliferation and activation markers corresponded to functional differences, we stimulated naive T cells with PMA and stained intracellularly for IFN-γ production. After 5 h of stimulation, a significantly higher frequency of Cmah$^{-/-}$ CD8 and CD4 T cells produced IFN-γ when compared with WT T cells (Fig. 1E). Similarly, Cmah$^{-/-}$ CD8 T cells stimulated for 5 h with an anti-CD3 Ab displayed a higher frequency of IFN-γ–producing T cells when compared with WT CD8 T cells (Supplemental Fig. 2B). Thus, Cmah$^{-/-}$ T cells more rapidly acquire an activated phenotype, proliferate faster, and produce more IFN-γ than WT T cells upon equivalent T cell stimulation in vitro.

Metabolically reintroducing Neu5Gc to Cmah$^{-/-}$ T cells and human T cells blunts proliferation and activation

Because both human T cells and Cmah$^{-/-}$ T cells lack the ability to produce Neu5Gc sialic acid, we hypothesized that metabolically reintroducing Neu5Gc into these cells (34) via the culture media would blunt the previously observed enhanced activation and proliferation. We activated CFSE-labeled human PBMCs and Cmah$^{-/-}$ mouse T cells for 5 d with immobilized anti-CD3 and soluble anti-CD28 in either Neu5Gc-containing media or Neu5Ac-containing control media. Efficient incorporation of Neu5Gc from the culture medium was visualized in human cells with an Ab recognizing Neu5Gc (Supplemental Fig. 2E). Both human and Cmah$^{-/-}$ T cell proliferation was blunted by the introduction of the missing Neu5Gc sialic acid when compared with control Neu5Ac fed T cells, as seen by decreased dilution of CFSE at 5 d postactivation (Fig. 2A). When we preincubated human CD4 T cells for 3 d in Neu5Gc-containing media and activated them for 2 d, they showed an ∼50% reduction in CD25 expression over Neu5Ac control fed T cells, indicating that Neu5Gc feeding of human T cells blunts activation (Fig. 2B). Similarly, preincubating Cmah$^{-/-}$ T cells for 2 d with Neu5Gc and activating them for 5 d greatly decreased activation marker CD69 levels in both CD4 and CD8 T cells when compared with Neu5Ac fed control T cells (Fig. 2B). These results indicate that the metabolic reintroduction of missing sialic acid Neu5Gc to both human and Cmah$^{-/-}$ T cells blunts their activation and proliferation during in vitro stimulation.

Cmah$^{-/-}$ mice mount a greater CD8 T cell response to AAV after Ad–AAV immunization

We hypothesized that the absence of CMAH in humans may have contributed to the unanticipated immune responses seen in AAV gene therapy trials (21–23). To test this, we moved to an in vivo viral immune challenge, to correlate the in vitro hyperactivation of Cmah$^{-/-}$ T cells to an in vivo phenotype. We i.m. immunized Cmah$^{-/-}$ and WT mice with a human Ad serotype 5 vector encoding the AAV serotype 2 capsid. No difference in AAV2-

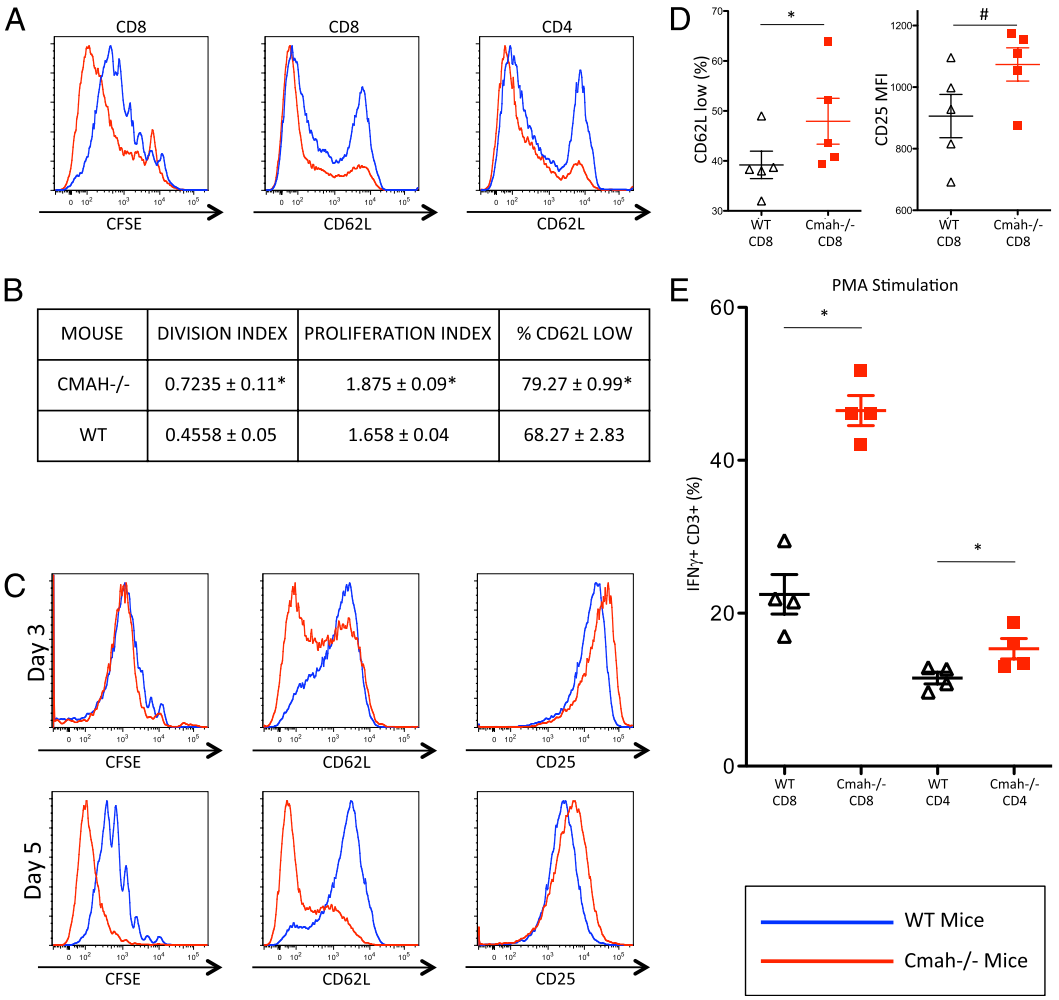

FIGURE 1. In vitro T cell proliferation and activation is augmented in Cmah$^{-/-}$ mice. (**A** and **C**) CFSE-labeled mouse splenocytes (A) or negatively isolated CD8$^+$ T cells (C) were activated in culture for 3 or 5 d with anti-CD3/anti-CD28 beads. Proliferation was assayed by visualizing CFSE dilution (*left panel*), whereas CD62L and CD25 expression were used to quantify activation differences (*middle* and *right panels*). Red shaded lines represent either representative Cmah$^{-/-}$ mice (A) or Cmah$^{-/-}$ isolated CD8$^+$ T cells (C), whereas blue shaded lines represent either representative WT mice (A) or WT isolated CD8$^+$ T cells (C). (**B**) CFSE-labeled mouse splenocytes were activated in culture for 5 d with anti-CD3/anti-CD28 beads. Proliferation indices and division indices on CD8 T cells were calculated based on analysis of CFSE dilution. (**D**) Mouse splenocytes were activated in culture for 5 h with anti-CD3/anti-CD28 beads and assayed for CD62L (*left panel*) and CD25 (*right panel*). (**E**) Mouse splenocytes were stimulated with PMA for 5 h and assayed for IFN-γ production. Black triangles represent WT cells; red squares represent Cmah$^{-/-}$ cells. $n = 5$ mice/group (A, B, D), pooled T cells isolated from 5 mice per group (C) and 4 mice per group (E). Results are representative of at least two experiments. $^*p \leq 0.05$, $^\#p < 0.1$, Student t test.

specific T cells was observed at baseline as expected (Fig. 3A), and no difference in naive T cell numbers was observed in the spleen of unimmunized mice (data not shown). However, a significantly higher number of T cells against the AAV2 capsid was found in the peripheral blood of Cmah$^{-/-}$ mice at day 10 when compared with WT mice (Fig. 3A). Although not as dramatic, an increase in Cmah$^{-/-}$ AAV2 capsid-specific T cells over WT T cells was also seen in day 10 splenocytes (Fig. 3B). In addition, when we stimulated day 10 splenocytes with the H-2K^b AAV2 peptide SNYNKSVNV, we observed a significantly higher frequency of Cmah$^{-/-}$ T cells producing IFN-γ when compared with WT T cells (Fig. 3C). Therefore, i.m. immunization with Ad-expressing AAV2 capsid leads to a more robust CD8 T cell response at day 10 in Cmah$^{-/-}$ mice versus WT mice.

Cmah$^{-/-}$ mice mount a greater T cell response during acute LCMV Armstrong infection

Although the Ad immunization results showed an enhanced T cell response in Cmah$^{-/-}$ mice, we sought to assess the T cell kinetics and activation during a live, replicating viral infection, predicting that Cmah$^{-/-}$ mice would mount a stronger T cell response during infection. To do this, we infected Cmah$^{-/-}$ mice and WT mice with the acute Armstrong strain of LCMV. Mice were bled longitudinally for PBMC analysis and sacrificed at day 42 for terminal splenocyte analysis. A representative flow cytometric gating strategy depicts how the data were analyzed (Supplemental Fig. 1). At the peak of the T cell response on day 8 postinfection, we observed a dramatic increase in the frequency of total CD8 T cells in the blood of Cmah$^{-/-}$ mice when compared with WT mice (Fig. 4A). We also observed significantly more Cmah$^{-/-}$ T cells directed against the gp33 epitope of LCMV at day 8 in the blood, and this difference remained significant throughout the duration of the 42-d study (Fig. 4B). Furthermore, we saw a marked increase in the number of LCMV-specific KLRG1-CD127$^+$ memory precursor T cells in Cmah$^{-/-}$ mice versus WT mice. This difference was apparent at day 14 postinfection and remained significant in the blood at day 42 (Fig. 4C). Interestingly, there was no difference in splenic LCMV viral titers during the course of the infection between Cmah$^{-/-}$ and WT mice (Supplemental Fig. 4). At day 42 postinfection, Cmah$^{-/-}$ mice also had a higher frequency

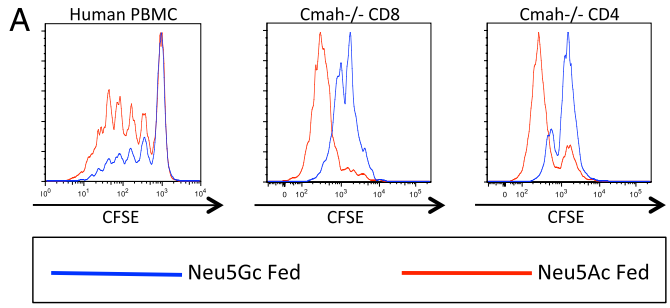

SAMPLE	DIVISION INDEX	PROLIFERATION INDEX
Human Ac	0.595	1.86
Human Gc	0.305	1.57
Cmah-/- CD8 Ac	1.98	3.2
Cmah-/- CD8 Gc	1.82	2.4
Cmah-/- CD4 Ac	2.35	2.78
Cmah-/- CD4 Gc	1.7	2.03

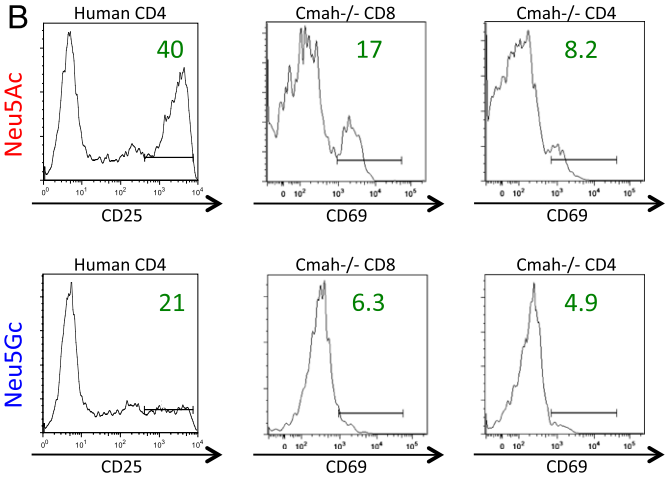

SAMPLE	CD25 MFI ON ACTIVATED CELLS	CD69 MFI ON ACTIVATED CELLS
Human Ac	3501	NA
Human Gc	2113	NA
Cmah-/- CD8 Ac	NA	2706
Cmah-/- CD8 Gc	NA	1828
Cmah-/- CD4 Ac	NA	1598
Cmah-/- CD4 Gc	NA	1500

FIGURE 2. Metabolically reintroducing Neu5Gc to Cmah$^{-/-}$ T cells and human T cells blunts proliferation and activation. (**A**) CFSE-labeled human PBMCs (*left panel*) or Cmah$^{-/-}$ mouse T cells pooled from five mice (*middle* and *right panels*) were stimulated with immobilized anti-CD3 and soluble anti-CD28 for 5 d in either Neu5Gc-containing media (blue line) or Neu5Ac-containing control media (red line), then collected and assayed for proliferation via CFSE dilution. Table on *right* summarizes the proliferation and division indices from these experiments. (**B**) Human CD4 T cells were preincubated in Neu5Gc or Neu5Ac media for 3 d, activated for 2 d as described earlier, and then assayed for activation via CD25 expression. Cmah$^{-/-}$ T cells were preincubated in Neu5Gc or Neu5Ac media for 2 d, activated for 5 d as described earlier, and then assayed for activation via CD69 expression. Table on *right* summarizes the mean fluorescent intensity of the assayed activation markers on positively expressing cells. Results are representative of at least three experiments on either pooled Cmah$^{-/-}$ mouse T cells (five mice) or individual human donors.

of LCMV-specific CD8 T cells in the spleen compared with WT mice (Fig. 4D), and a higher frequency of these LCMV-specific T cells were memory precursor KLRG1-CD127^{+} (Fig. 4E). In an attempt to determine whether the in vivo response to LCMV is CD8 autonomous, we transferred 20E6 CD8 T cells from either Cmah$^{-/-}$ or WT mice into congenic Ly5.1 mice. Because Cmah$^{-/-}$ and WT littermates are on a C57BL/6 background, they are Ly5.2^{+} and can be tracked in the Ly5.1 recipient mice. Recipient mice were infected with LCMV and sacrificed at days 6–7 to analyze PBMCs and splenocytes. We observed greater numbers of Cmah$^{-/-}$ gp33^{+} donor CD8 T cells in the spleen and a trend for greater numbers in the PBMCs when compared with the response of WT CD8 T cells in recipient mice (Fig. 4F). This supports the hypothesis that the observed CD8 T cell response to LCMV infection is CD8 autonomous. Thus, after a live viral infection with LCMV, Cmah$^{-/-}$ mice generate a greater number of LCMV-specific T cells in the blood and spleen compared with WT mice. In addition, a greater proportion of the Cmah$^{-/-}$ LCMV-specific T cell compartment is composed of KLRG1-CD127^{+} memory precursor cells.

LCMV-specific T cells in Cmah$^{-/-}$ mice produce a higher proportion of cytokines than WT T cells

We also hypothesized that T cells generated against LCMV were themselves more functional in Cmah$^{-/-}$ mice versus WT mice. To test this, we stimulated equal numbers of day 42 splenocytes from Cmah$^{-/-}$ and WT mice with LCMV peptides and stained for intracellular cytokine production. We observed a higher proportion of IFN-γ^{+} Mip1α^{+} T cells in Cmah$^{-/-}$ mice compared with WT mice (Fig. 5A, 5B), which correlated well with the observed increase in LCMV-specific T cells by tetramer staining. To assess the polyfunctionality of the CD8 T cell compartment, we looked at production of TNF-α and IL-2 by the IFN-γ^{+} Mip1α^{+} T cells. A significantly greater proportion of Cmah$^{-/-}$ Mip1α^{+}IFN-γ^{+} CD8 T cells made both TNF-α and IL-2 when compared with WT CD8 T cells (Fig. 5C). Similar trends in increased T cell functionality were observed in day 8 splenocytes (Supplemental Fig. 3). Furthermore, Cmah$^{-/-}$ mice had an increase in the proportion of day 42 CD8 T cells capable of performing multiple functions simultaneously (expression of CD107a, Mip1α, IFN-γ, TNF-α, and IL-2) upon peptide stimulation. This was especially evident in the fraction of CD8 T cells that produced four or five functions simultaneously (Fig. 5D, 5E). In summary, the T cell response to LCMV Armstrong in Cmah$^{-/-}$ mice is more robust than the response seen in WT mice.

Discussion

Several theories have been proposed to explain the loss of function of the CMAH enzyme in humans after their evolutionary divergence from nonhuman hominids. One holds that a pathogen that bound Neu5Gc sialic acid may have been so detrimental to human survival that the mutation of CMAH, and thus the loss of Neu5Gc expression, allowed humans to escape this pathogen (7, 35). This would have placed an enormous benefit on fixing this mutation in the human population, perhaps even at the cost of reduced inter-

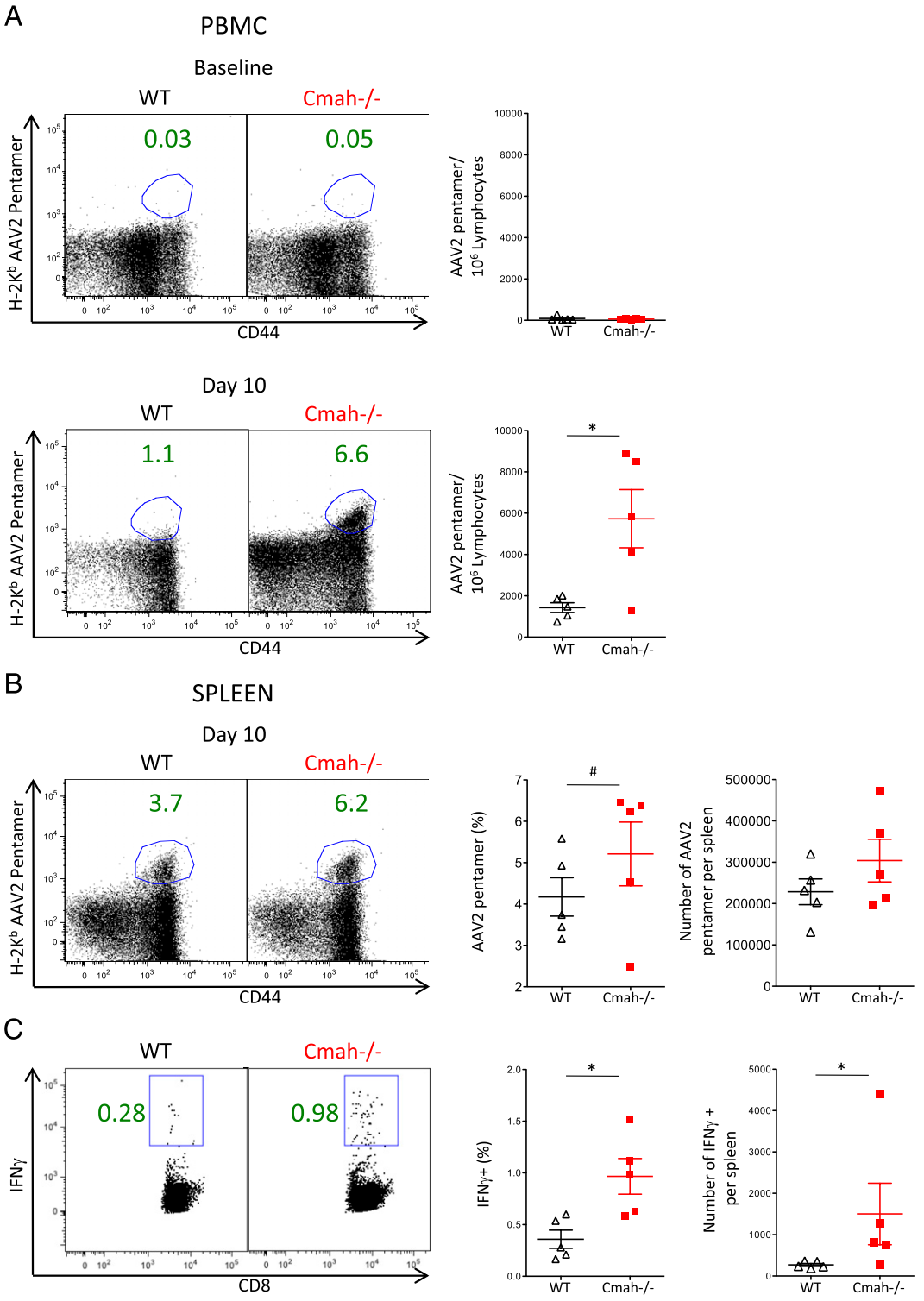

FIGURE 3. Cmah$^{-/-}$ mice mount a greater CD8 T cell response to AAV after Ad–AAV immunization. Mice were immunized with human Ad serotype 5 i.m. (**A**) Representative frequency of H-2K^b AAV2-Pentamer$^+$ CD8$^+$ T cells in the blood at baseline (*top*) and day 10 (*bottom*) of WT (*left panels*) and Cmah$^{-/-}$ (*middle panels*) mice and the number of H-2K^b AAV2-Pentamer$^+$ CD8$^+$ T cells per IE6 lymphocytes (*right panels*). (**B**) Representative frequency of H-2K^b AAV2-Pentamer$^+$ CD8$^+$ T cells in the spleen at day 10 of WT (*left panel*) and Cmah$^{-/-}$ (*middle left panel*) mice and the frequency of H-2K^b AAV2-Pentamer$^+$ CD8$^+$ T cells (*middle right panel*). Absolute numbers of H-2K^b AAV2-Pentamer$^+$ CD8$^+$ T cells are plotted in the *far right panel*. (**C**) Representative frequency of IFN-γ$^+$ CD8 T cells in day 10 spleens of WT (*left panel*) and Cmah$^{-/-}$ (*middle left panel*) mice after 5 h of H-2K^b AAV2 peptide SNYNKSVNV stimulation and the summary plot of all frequencies in each group (*middle right panel*). Absolute numbers of IFN-γ$^+$ CD8 T cells are plotted in the *far right panel*. $n = 5$ mice/group. Results are representative of at least two experiments. $^*p < 0.05$, $^\#p < 0.1$, Student t test.

action of glycans with ITIM-bearing inhibitory receptors and altered immunologic effects.

In our study, we showed that Cmah$^{-/-}$ mouse T cells had higher levels of activation markers and proliferated faster in vitro upon equivalent stimulation when compared with WT mice. These results are similar to studies done in human versus chimpanzee T cells, where human T cells proliferate more than equivalently stimulated chimpanzee T cells (19, 20). In those human versus chimpanzee

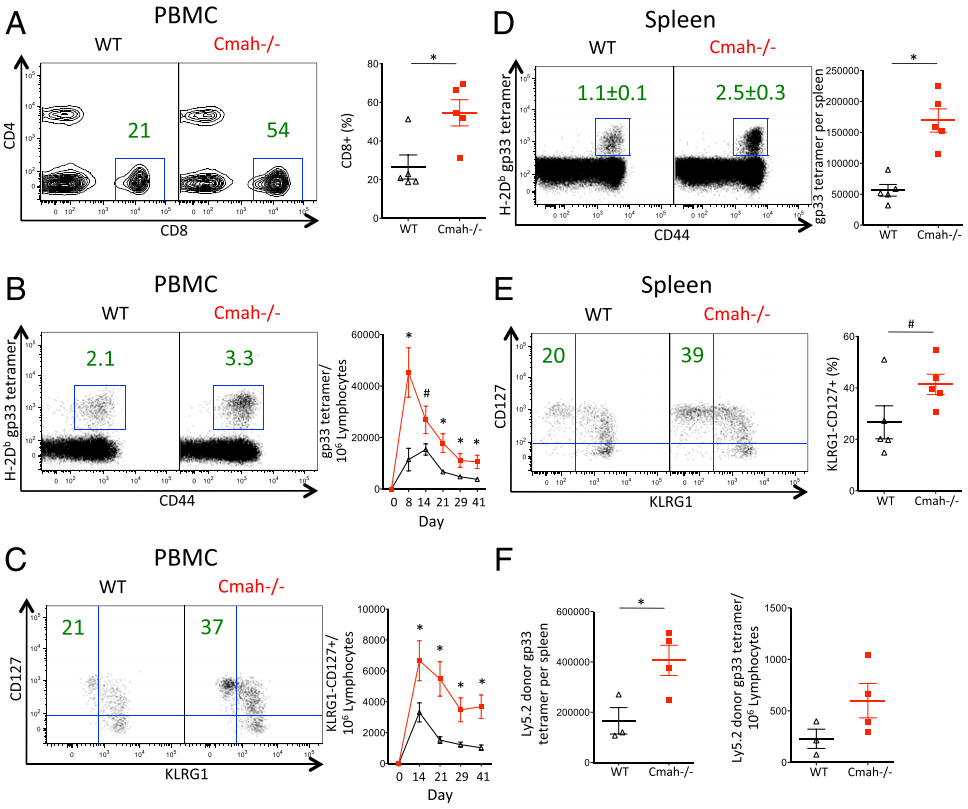

FIGURE 4. Cmah$^{-/-}$ mice mount a greater T cell response during acute LCMV Armstrong infection. Mice were infected with acute LCMV strain Armstrong and bled at various time points until sacrifice and spleen isolation at day 42. (**A**–**C**) Mouse PBMCs. (A) Frequency of CD8$^+$ T cells at day 8 in the blood of WT (*left plot* and black triangles in *right plot*) and Cmah$^{-/-}$ (*middle plot* and red squares in *right plot*) mice. *Left* and *middle plots* show the median representative dot plots from each group, whereas the *right plot* shows quantification of the frequencies. (B) Number of LCMV H2-D^b gp33 tetramer$^+$ CD8$^+$ T cells per 1E6 lymphocytes in the blood of WT (black line, *right plot*) and Cmah$^{-/-}$ (red line, *right plot*) mice over 42 d. *Left* and *middle plots* show the median representative dot plots from day 42 from each group, whereas the *right plot* graphs the number of tetramer$^+$ cells per 1E6 lymphocytes over time. (C) Number of LCMV H2-D^b gp33 tetramer$^+$ CD8$^+$ T cells that are KLRG1-CD127$^+$ per 1E6 lymphocytes in the blood of WT (black line, *right plot*) and Cmah$^{-/-}$ (red line, *right plot*) mice over 42 d. *Left* and *middle plots* show the median representative dot plots from day 42 from each group, whereas the *right plot* graphs the number of memory-phenotype tetramer$^+$ cells per 1E6 lymphocytes over time. (**D** and **E**) Mouse splenocytes at day 42. (D) *Left* and *middle plots* show the median representative dot plots of the frequencies of LCMV H2-D^b gp33 tetramer$^+$ CD8$^+$ splenocytes from day 42 from each group, whereas the *right plot* shows quantification of the absolute numbers of these cells in the spleen. WT (black triangles in *right plot*) and Cmah$^{-/-}$ (red squares in *right plot*). Similar trends were observed in the number of gp276 tetramer$^+$ CD8$^+$ splenocytes. (E) *Left* and *middle plots* show the median representative dot plots of the frequencies of KLRG1-CD127$^+$ LCMV H2-D^b gp33 tetramer$^+$ CD8$^+$ splenocytes, whereas the plot on the *right* shows quantification of these frequencies in WT (black triangles in *right plot*) and Cmah$^{-/-}$ (red squares in *right plot*) spleens. (**F**) Day 7 CD8 donor (Ly5.2) analysis in Ly5.1 recipient mice infected with LCMV. *Left plot* shows the number of gp33$^+$ CD8$^+$ donor T cells per spleen and *right plot* shows the number of gp33$^+$ CD8$^+$ donor T cells per 1E6 lymphocytes in the blood. Cmah$^{-/-}$ (red squares, four mice), WT (black triangles, three mice). $n = 5$ mice/group (A–E). Results are representative of at least two experiments. $^*p < 0.05$, $^\#p < 0.1$, Student t test.

studies, it was hypothesized that the loss of Siglecs on human T cells, likely a result of evolution from the loss of CMAH function, reduced the inhibitory threshold for activation. Accordingly, Siglec-5 transfection of human T cells was able to blunt the proliferation effect. In our study, we metabolically reintroduced Neu5Gc sialic acid via the culture media of both human and Cmah$^{-/-}$ T cells, and observed reduced proliferation and activation.

The observed blunting of proliferation and activation upon Neu5Gc feeding fits well with a recent study that reported a physiologic reduction of CMAH function and Neu5Gc expression during normal murine T cell activation (30). This article showed decreased binding of activated T cells to several ITIM-bearing Siglecs, including CD22, a known B cell inhibitory Siglec that preferentially binds Neu5Gc. Less clear is the presence of these Siglecs on murine T cells, with the exception of one study that showed CD22 on some murine T cells (36). Indeed, we confirmed that CD22 is both transcribed and expressed on WT and Cmah$^{-/-}$ T cells, albeit on a subset of the total population (data not shown). Therefore, the loss of Neu5Gc may have rendered these cells more readily activated, because there would be less CD22 (and thus less associated phosphatase activity) clustering with sialylated receptors at the surface. Although this may be a suitable explanation for the subset of cells expressing CD22, we cannot conclude that this is entirely responsible for the observed proliferation and activation differences. Future studies should focus on additional identification of Siglecs on murine T cells, whether there are membrane steric or electric charge effects due to the additional oxygen atom in Neu5Gc sialic acid, and whether there are differences in the turnover of these sialic acids on the cell surface under varying physiologic conditions.

When we challenged mice in vivo with a live, replicating acute strain of LCMV (Armstrong), Cmah$^{-/-}$ mice generated greater numbers of CD8 T cells directed against the LCMV virus. The higher frequencies of LCMV-specific T cells are likely a result of reduced activation thresholds and corroborate the observed increases in proliferation and activation in vitro. Previous studies have shown that a long-lived memory T cell population arises from a killer cell lectin-like receptor G1 (KLRG1) low, IL-7Rα (CD127) high subset of Ag-specific cells (37, 38). Interestingly, among the

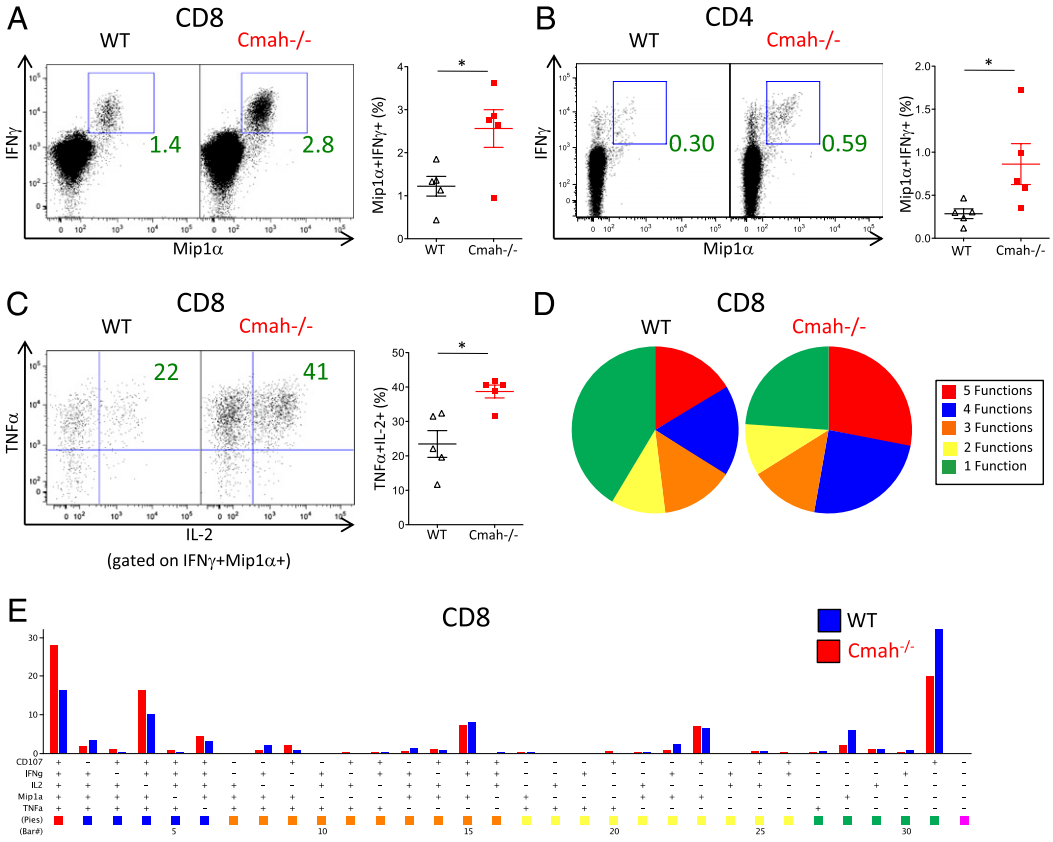

FIGURE 5. LCMV-specific T cells in Cmah$^{-/-}$ mice produce a higher proportion of cytokines than WT T cells. Mice infected with acute LCMV Armstrong were sacrificed at day 42, and isolated splenocytes were stimulated for 5 h with LCMV peptides and stained for multiple cytokines to assay functionality. (**A** and **C**–**E**) Functionality of CD8$^+$ T cells upon LCMV peptide GP276 stimulation. (A) Frequency of Mip1α$^+$IFN-γ$^+$ CD8$^+$ T cells upon LCMV peptide stimulation in WT (black triangles in *right plot*) and Cmah$^{-/-}$ (red squares in right *plot*) mice. *Left* and *middle plots* show the median representative dot plots from each group, whereas the *right* plot shows the quantification of the frequencies. (**B**) Frequency of Mip1α$^+$IFN-γ$^+$ CD4$^+$ T cells upon LCMV peptide GP66-77 stimulation in WT (black triangles in *right plot*) and Cmah$^{-/-}$ (red squares in *right plot*) mice. *Left* and *middle plots* show the median representative dot plots from each group, whereas the right plot shows the quantification of the frequencies. (C) Frequency of Mip1α$^+$IFN-γ$^+$ CD8$^+$ T cells from (A) that are TNF-α$^+$IL-2$^+$. Representative plots on the *left* and *middle*; quantification on the right as described in (A). (D) Polyfunctional pie charts of day 42 stimulated CD8$^+$ T cells from WT (*left* pie chart) and Cmah$^{-/-}$ (*right* pie chart) mice. Red = 5 functions, blue = 4 functions, orange = 3 functions, yellow = 2 functions, green = 1 function. Functions = CD107a, Mip1α, IFN-γ, TNF-α, and IL-2. (E) Bar graph representation of each combination of the functions defined in (D) between WT (blue bars) and Cmah$^{-/-}$ (red bars) CD8$^+$ T cells, with the corresponding pie chart color on the bottom. n = 5 mice/group. Results are representative of at least two experiments. *$p < 0.05$, Student t test.

LCMV-specific T cells, there was a higher frequency of KLRG1-CD127$^+$ memory-precursor T cells in Cmah$^{-/-}$ mice. This precursor difference did not seem to be due to a difference in LCMV viral load kinetics in the spleen at days 3, 5, and 7 (Supplemental Fig. 4). It remains possible that even a minor change in Ag level that we may not have detected could have led to differences in memory formation, as Ag removal is known to lead to memory transition of T cells (39). Other factors known to influence memory T cell formation include CD4 T cell help (40), the strength and duration of TCR stimulation (39, 41, 42), inflammation during T cell activation (39, 41), and clonal competition (42). Although we observed enhanced CD4 responses in Cmah$^{-/-}$ mice, it is unclear whether this affected the quantity of memory precursor cells. We additionally observed qualitatively enhanced CD8 responses at day 42 in Cmah$^{-/-}$ mouse splenocytes. These CD8 cells were highly polyfunctional upon LCMV peptide stimulation, simultaneously degranulating and producing high levels of IFN-γ, TNF-α, and IL-2, a hallmark of memory T cells. We therefore conclude that Cmah$^{-/-}$ mice make a more functional response upon LCMV Ag stimulation at a memory time point when compared with WT littermate mice.

We also showed that Cmah$^{-/-}$ mice immunized with an Ad vector encoding the AAV capsid mounted a greater T cell response to the AAV capsid transgene when compared with WT mice. This finding is of particular relevance to recent clinical results in trials of AAV-mediated gene transfer of factor IX to the liver of men with severe hemophilia B. Animal gene transfer models had failed to predict a T cell–mediated immune response directed against the AAV capsid that resulted in transient elevation in liver enzymes and a loss of the donated gene in patients with severe hemophilia (21, 22). Subsequent attempts to develop an animal model that accurately mimicked the observed T cell responses in humans were unsuccessful (24–26, 43). The generally accepted hypothesis accounting for immune responses generated against the AAV vector in humans is that a preexisting memory pool of T cells from an early childhood infection is reactivated upon gene transfer and attacks virally infected cells (44). Although it is certainly the case that most preclinical animal studies were performed in naive hosts, NHPs are also natural hosts for AAV. It has been shown that despite the presence of CD8 T cells specific for AAV in NHP, humans have a more polyfunctional resident memory population of AAV-specific T cells, whereas NHP have a population of CD8 T cells with an effector cell phenotype that seems to be less functional upon stimulation (45). In preclinical gene transfer studies in which NHPs

were infused with AAV, there was no observed T cell response or transaminitis (46–48).

To put our results in a wider context, there are many instances of what might be termed inappropriate immune responses in human pathology, including autoimmune disease, chronic inflammation, and the progression of HIV infection to AIDS. These pathologic conditions are not as frequent in other species and, for research purposes, are generally experimentally induced, because they are not naturally occurring. Many changes over human evolution have likely contributed to the presently heightened immune response in humans compared with other species. However, our findings of augmented T cell responses, in a mouse with a uniquely human glycosylation mutation likely to alter binding to ITIM-bearing inhibitory receptors, highlight the relationship between glycosylation and immune regulation in human pathology.

Acknowledgments

We acknowledge Robert Davidson for assistance with animal procedures and Dr. Sarah Ratcliffe for helpful discussion on statistical analysis. We also acknowledge Drs. Robert H. Vonderheide, Michael R. Betts, Kyong-Mi Chang, and all members of the High, Wherry, Koretzky, and Varki laboratories for helpful comments and discussion.

Disclosures

The authors have no financial conflicts of interest.

References

1. Varki, A., and J. B. Lowe. 2009. Biological roles of glycans. In *Essentials of Glycobiology*, 2nd Ed. A. Varki, R. D. Cummings, J. D. Esko, H. H. Freeze, P. Stanley, C. R. Bertozzi, G. W. Hart, and M. E. Etzler, eds. Cold Spring Harbor Laboratory Press, Cold Spring Harbor, NY.
2. Chou, H. H., H. Takematsu, S. Diaz, J. Iber, E. Nickerson, K. L. Wright, E. A. Muchmore, D. L. Nelson, S. T. Warren, and A. Varki. 1998. A mutation in human CMP-sialic acid hydroxylase occurred after the *Homo-Pan* divergence. *Proc. Natl. Acad. Sci. USA* 95: 11751–11756.
3. Irie, A., S. Koyama, Y. Kozutsumi, T. Kawasaki, and A. Suzuki. 1998. The molecular basis for the absence of N-glycolylneuraminic acid in humans. *J. Biol. Chem.* 273: 15866–15871.
4. Brinkman-Van der Linden, E. C., E. R. Sjoberg, L. R. Juneja, P. R. Crocker, N. Varki, and A. Varki. 2000. Loss of N-glycolylneuraminic acid in human evolution. Implications for sialic acid recognition by siglecs. *J. Biol. Chem.* 275: 8633–8640.
5. Tangvoranuntakul, P., P. Gagneux, S. Diaz, M. Bardor, N. Varki, A. Varki, and E. Muchmore. 2003. Human uptake and incorporation of an immunogenic nonhuman dietary sialic acid. *Proc. Natl. Acad. Sci. USA* 100: 12045–12050.
6. Varki, A. 2010. Colloquium paper: uniquely human evolution of sialic acid genetics and biology. *Proc. Natl. Acad. Sci. USA* 107(Suppl. 2): 8939–8946.
7. Varki, N. M., E. Strobert, E. J. Dick, Jr., K. Benirschke, and A. Varki. 2011. Biomedical differences between human and nonhuman hominids: potential roles for uniquely human aspects of sialic acid biology. *Annu. Rev. Pathol.* 6: 365–393.
8. Crocker, P. R., J. C. Paulson, and A. Varki. 2007. Siglecs and their roles in the immune system. *Nat. Rev. Immunol.* 7: 255–266.
9. Varki, A., and P. R. Crocker. 2009. I-type lectins. In *Essentials of Glycobiology*, 2nd Ed. A. Varki, R. D. Cummings, J. D. Esko, H. H. Freeze, P. Stanley, C. R. Bertozzi, G. W. Hart, and M. E. Etzler, eds. Cold Spring Harbor Laboratory Press, Cold Spring Harbor, NY.
10. Ravetch, J. V., and L. L. Lanier. 2000. Immune inhibitory receptors. *Science* 290: 84–89.
11. Collins, B. E., O. Blixt, A. R. DeSieno, N. Bovin, J. D. Marth, and J. C. Paulson. 2004. Masking of CD22 by cis ligands does not prevent redistribution of CD22 to sites of cell contact. *Proc. Natl. Acad. Sci. USA* 101: 6104–6109.
12. Doody, G. M., L. B. Justement, C. C. Delibrias, R. J. Matthews, J. Lin, M. L. Thomas, and D. T. Fearon. 1995. A role in B cell activation for CD22 and the protein tyrosine phosphatase SHP. *Science* 269: 242–244.
13. Taylor, V. C., C. D. Buckley, M. Douglas, A. J. Cody, D. L. Simmons, and S. D. Freeman. 1999. The myeloid-specific sialic acid-binding receptor, CD33, associates with the protein-tyrosine phosphatases, SHP-1 and SHP-2. *J. Biol. Chem.* 274: 11505–11512.
14. Vitale, C., C. Romagnani, M. Falco, M. Ponte, M. Vitale, A. Moretta, A. Bacigalupo, L. Moretta, and M. C. Mingari. 1999. Engagement of p75/AIRM1 or CD33 inhibits the proliferation of normal or leukemic myeloid cells. *Proc. Natl. Acad. Sci. USA* 96: 15091–15096.
15. Ikehara, Y., S. K. Ikehara, and J. C. Paulson. 2004. Negative regulation of T cell receptor signaling by Siglec-7 (p70/AIRM) and Siglec-9. *J. Biol. Chem.* 279: 43117–43125.
16. Hoffmann, A., S. Kerr, J. Jellusova, J. Zhang, F. Weisel, U. Wellmann, T. H. Winkler, B. Kneitz, P. R. Crocker, and L. Nitschke. 2007. Siglec-G is a B1 cell-inhibitory receptor that controls expansion and calcium signaling of the B1 cell population. *Nat. Immunol.* 8: 695–704.
17. Yu, Z., M. Maoui, L. Wu, D. Banville, and S. Shen. 2001. mSiglec-E, a novel mouse CD33-related siglec (sialic acid-binding immunoglobulin-like lectin) that recruits Src homology 2 (SH2)-domain-containing protein tyrosine phosphatases SHP-1 and SHP-2. *Biochem. J.* 353: 483–492.
18. Zhang, M., T. Angata, J. Y. Cho, M. Miller, D. H. Broide, and A. Varki. 2007. Defining the in vivo function of Siglec-F, a CD33-related Siglec expressed on mouse eosinophils. *Blood* 109: 4280–4287.
19. Nguyen, D. H., N. Hurtado-Ziola, P. Gagneux, and A. Varki. 2006. Loss of Siglec expression on T lymphocytes during human evolution. *Proc. Natl. Acad. Sci. USA* 103: 7765–7770.
20. Soto, P. C., L. L. Stein, N. Hurtado-Ziola, S. M. Hedrick, and A. Varki. 2010. Relative over-reactivity of human versus chimpanzee lymphocytes: implications for the human diseases associated with immune activation. *J. Immunol.* 184: 4185–4195.
21. Manno, C. S., G. F. Pierce, V. R. Arruda, B. Glader, M. Ragni, J. J. Rasko, M. C. Ozelo, K. Hoots, P. Blatt, B. Konkle, et al. 2006. Successful transduction of liver in hemophilia by AAV-Factor IX and limitations imposed by the host immune response. [Published erratum appears in 2006 *Nat. Med.* 12: 592.] *Nat. Med.* 12: 342–347.
22. Nathwani, A. C., E. G. D. Tuddenham, S. Rangarajan, C. Rosales, J. McIntosh, D. C. Linch, P. Chowdary, A. Riddell, A. J. Pie, C. Harrington, et al. 2011. Adenovirus-associated virus vector-mediated gene transfer in hemophilia B. *N. Engl. J. Med.* 365: 2357–2365.
23. Mingozzi, F., M. V. Maus, D. J. Hui, D. E. Sabatino, S. L. Murphy, J. E. J. Rasko, M. V. Ragni, C. S. Manno, J. Sommer, H. Jiang, et al. 2007. CD8(+) T-cell responses to adeno-associated virus capsid in humans. *Nat. Med.* 13: 419–422.
24. Li, H., S. L. Murphy, W. Giles-Davis, S. Edmonson, Z. Xiang, Y. Li, M. O. Lasaro, K. A. High, and H. C. Ertl. 2007. Pre-existing AAV capsid-specific CD8+ T cells are unable to eliminate AAV-transduced hepatocytes. *Mol. Ther.* 15: 792–800.
25. Wang, L., J. Figueredo, R. Calcedo, J. Lin, and J. M. Wilson. 2007. Cross-presentation of adeno-associated virus serotype 2 capsids activates cytotoxic T cells but does not render hepatocytes effective cytolytic targets. *Hum. Gene Ther.* 18: 185–194.
26. Li, C., M. Hirsch, N. DiPrimio, A. Asokan, K. Goudy, R. Tisch, and R. J. Samulski. 2009. Cytotoxic-T-lymphocyte-mediated elimination of target cells transduced with engineered adeno-associated virus type 2 vector in vivo. *J. Virol.* 83: 6817–6824.
27. Hedlund, M., P. Tangvoranuntakul, H. Takematsu, J. M. Long, G. D. Housley, Y. Kozutsumi, A. Suzuki, A. Wynshaw-Boris, A. F. Ryan, R. L. Gallo, et al. 2007. N-glycolylneuraminic acid deficiency in mice: implications for human biology and evolution. *Mol. Cell. Biol.* 27: 4340–4346.
28. Naito, Y., H. Takematsu, S. Koyama, S. Miyake, H. Yamamoto, R. Fujinawa, M. Sugai, Y. Okuno, G. Tsujimoto, T. Yamaji, et al. 2007. Germinal center marker GL7 probes activation-dependent repression of N-glycolylneuraminic acid, a sialic acid species involved in the negative modulation of B-cell activation. *Mol. Cell. Biol.* 27: 3008–3022.
29. Chandrasekharan, K., J. H. Yoon, Y. Xu, S. deVries, M. Camboni, P. M. L. Janssen, A. Varki, and P. T. Martin. 2010. A human-specific deletion in mouse Cmah increases disease severity in the mdx model of duchenne muscular dystrophy. *Sci. Transl. Med.* 2: 42ra54.
30. Redelinghuys, P., A. Antonopoulos, Y. Liu, M. A. Campanero-Rhodes, E. McKenzie, S. M. Haslam, A. Dell, T. Feizi, and P. R. Crocker. 2011. Early murine T-lymphocyte activation is accompanied by a switch from N-Glycolyl- to N-acetyl-neuraminic acid and generation of ligands for siglec-E. *J. Biol. Chem.* 286: 34522–34532.
31. Pearce, O. M. T., and A. Varki. 2010. Chemo-enzymatic synthesis of the carbohydrate antigen N-glycolylneuraminic acid from glucose. *Carbohydr. Res.* 345: 1225–1229.
32. Sabatino, D. E., F. Mingozzi, D. J. Hui, H. Chen, P. Colosi, H. C. J. Ertl, and K. A. High. 2005. Identification of mouse AAV capsid-specific CD8+ T cell epitopes. *Mol. Ther.* 12: 1023–1033.
33. Ahmed, R., A. Salmi, L. D. Butler, J. M. Chiller, and M. B. Oldstone. 1984. Selection of genetic variants of lymphocytic choriomeningitis virus in spleens of persistently infected mice. Role in suppression of cytotoxic T lymphocyte response and viral persistence. *J. Exp. Med.* 160: 521–540.
34. Bardor, M., D. H. Nguyen, S. Diaz, and A. Varki. 2005. Mechanism of uptake and incorporation of the non-human sialic acid N-glycolylneuraminic acid into human cells. *J. Biol. Chem.* 280: 4228–4237.
35. Varki, A., and P. Gagneux. 2009. Human-specific evolution of sialic acid targets: explaining the malignant malaria mystery? *Proc. Natl. Acad. Sci. USA* 106: 14739–14740.
36. Sathish, J. G., J. Walters, J. C. Luo, K. G. Johnson, F. G. Leroy, P. Brennan, K. P. Kim, S. P. Gygi, B. G. Neel, and R. J. Matthews. 2004. CD22 is a functional ligand for SH2 domain-containing protein-tyrosine phosphatase-1 in primary T cells. *J. Biol. Chem.* 279: 47783–47791.
37. Sarkar, S., V. Kalia, W. N. Haining, B. T. Konieczny, S. Subramaniam, and R. Ahmed. 2008. Functional and genomic profiling of effector CD8 T cell subsets with distinct memory fates. *J. Exp. Med.* 205: 625–640.
38. Jung, Y. W., R. L. Rutishauser, N. S. Joshi, A. M. Haberman, and S. M. Kaech. 2010. Differential localization of effector and memory CD8 T cell subsets in lymphoid organs during acute viral infection. *J. Immunol.* 185: 5315–5325.

39. Kaech, S. M., and E. J. Wherry. 2007. Heterogeneity and cell-fate decisions in effector and memory CD8+ T cell differentiation during viral infection. *Immunity* 27: 393–405.
40. Wherry, E. J., and R. Ahmed. 2004. Memory CD8 T-cell differentiation during viral infection. *J. Virol.* 78: 5535–5545.
41. Jameson, S. C., and D. Masopust. 2009. Diversity in T cell memory: an embarrassment of riches. *Immunity* 31: 859–871.
42. Sarkar, S., V. Teichgräber, V. Kalia, A. Polley, D. Masopust, L. E. Harrington, R. Ahmed, and E. J. Wherry. 2007. Strength of stimulus and clonal competition impact the rate of memory CD8 T cell differentiation. *J. Immunol.* 179: 6704–6714.
43. Li, H., S.-W. Lin, W. Giles-Davis, Y. Li, D. Zhou, Z. Q. Xiang, K. A. High, and H. C. J. Ertl. 2009. A preclinical animal model to assess the effect of pre-existing immunity on AAV-mediated gene transfer. *Mol. Ther.* 17: 1215–1224.
44. Mingozzi, F., and K. A. High. 2011. Therapeutic in vivo gene transfer for genetic disease using AAV: progress and challenges. *Nat. Rev. Genet.* 12: 341–355.
45. Li, H., M. O. Lasaro, B. Jia, S.-W. Lin, L. H. Haut, K. A. High, and H. C. J. Ertl. 2011. Capsid-specific T-cell responses to natural infections with adeno-associated viruses in humans differ from those of nonhuman primates. *Mol. Ther.* 19: 2021–2030.
46. Mingozzi, F., N. C. Hasbrouck, E. Basner-Tschakarjan, S. A. Edmonson, D. J. Hui, D. E. Sabatino, S. Zhou, J. F. Wright, H. Jiang, G. F. Pierce, et al. 2007. Modulation of tolerance to the transgene product in a nonhuman primate model of AAV-mediated gene transfer to liver. *Blood* 110: 2334–2341.
47. Nathwani, A. C., J. T. Gray, J. McIntosh, C. Y. C. Ng, J. Zhou, Y. Spence, M. Cochrane, E. Gray, E. G. D. Tuddenham, and A. M. Davidoff. 2007. Safe and efficient transduction of the liver after peripheral vein infusion of self-complementary AAV vector results in stable therapeutic expression of human FIX in nonhuman primates. *Blood* 109: 1414–1421.
48. Nathwani, A. C., C. Rosales, J. McIntosh, G. Rastegarlari, D. Nathwani, D. Raj, S. Nawathe, S. N. Waddington, R. Bronson, S. Jackson, et al. 2011. Long-term safety and efficacy following systemic administration of a self-complementary AAV vector encoding human FIX pseudotyped with serotype 5 and 8 capsid proteins. *Mol. Ther.* 19: 876–885.

SUPPLEMENTAL:

SUPPLEMENTAL FIGURE LEGENDS

Supplemental Figure 1: Gating Strategy for Flow Cytometric Analysis. General gating schemes for the live viral infection analyses throughout the manuscript. Cells were plotted forward scatter area vs. side scatter area to determine the lymphocyte population (top left). After gating on the lymphocyte population, gates were subsequently made to only include singlets(top middle) and live cells(top right). Then CD8+ cells were selected (middle left) and either plotted for tetramer response or for cytokine analysis and IFNγ production.

Supplemental Figure 2: Additional In Vitro Proliferation Data. (A, C-D,F) CFSE-labeled mouse splenocytes were activated in culture for 5 days with α-CD3 α-CD28 beads. Proliferation was assayed by visualizing CFSE dilution, while CD62L expression was used to quantify activation differences. Red-shaded lines show representative Cmah-/- mice while blue-shaded lines show representative WT mice. (A) CD4 T cells activated for 5 days and assayed for CFSE dilution. (B)Mouse splenocytes were stimulated with α-CD3 antibody for 5 hours in culture and assayed intracellularly for IFNγ production. (C) Unstimulated, CFSE labeled splenocytes plated for 5 days to show baseline CFSE dilution. (D) Unstimulated CD8 T cells assayed for baseline CD62L levels prior to stimulation. (E) Isolated human PBMC were stimulated with α-CD3 α-CD28 in the presence of 3mM Neu5Gc-containing or Neu5Ac-containing media for 5 days. Neu5Gc levels were assayed by flow cytometry with a chicken-anti-Neu5Gc primary antibody followed by a Cy5 conjugated anti-chicken secondary antibody. Blue line-Neu5Gc fed cells, red line-Neu5Ac fed cells. (F) Percent death of day 5 stimulated Cmah-/- and WT CD8 T cells. *$p<0.05$, student's t test.

Supplemental Figure 3: LCMV-specific T Cells in Cmah-/- Produce a Higher Proportion of Cytokines Than WT T Cells at Day 8 in the Spleen. Mice infected with acute LCMV Armstrong were sacrificed at day 8, and isolated splenocytes were stimulated for 5 hours with LCMV peptides and stained for multiple cytokines to assay functionality. (A and B) Functionality of CD8+ T cells upon LCMV peptide GP276 stimulation. (A) Frequency of CD107a+IFNγ+ CD8+ T cells upon LCMV peptide stimulation in WT(black triangles in right plot) and Cmah-/-(red squares in right plot) mice. Left and middle plots show the median representative dot plots from each group, while the right plot shows the quantification of the frequencies. (B) Frequency of CD107a+IFNγ+ CD8+ T cells from (A) that are Mip1α+TNFα+. Representative plots on the left and middle, quantification on the right as described in (A). (C and D) Functionality of CD4+ T cells upon LCMV peptide GP66-77 stimulation. (C) Frequency of CD107a+IFNγ+ CD4+ T cells upon peptide stimulation in WT(black triangles in right plot) and Cmah-/-(red squares in right plot) mice. Left and middle plots show the median representative dot plots from each group, while

the right plot shows the quantification of the frequencies. (D) Frequency of CD107a+IFNγ+ CD4+ T cells from (D) that are Mip1α+TNFα+. Representative plots on the left and middle, quantification on the right as described in (D). N=5 mice per group. *p<0.05, student's t test.

Supplemental Figure 4: LCMV Armstrong Splenic Viral Titer Kinetics are Similar in WT and Cmah-/- Mice. Mice infected with acute LCMV Armstrong were sacrificed at days 3, 5, and 7, and spleens were homogenized and used in viral plaque assays to determine titer kinetics in WT(black triangles) and Cmah-/-(red squares) mice. L.O.D.=limit of detection. Day 3 and 5: 4 WT and 5 Cmah-/- mice, day 7: 5 WT and 5 Cmah-/- mice.